科学通报 2017 年 第 62 卷 第 6 期: 478 ~ 485
专辑: 胶体与界面化学 进 展
《中国科学》杂志社
SCIENCE CHINA PRESS

离子液体中构建溶致液晶

李钦堂, 陈晓*

山东大学胶体与界面化学教育部重点实验室, 济南 250100
* 联系人, E-mail: xchen@sdu.edu.cn

2016-03-21 收稿, 2016-04-12 修回, 2016-04-13 接受, 2016-05-25 网络版发表
国家自然科学基金(20973104, 21373127)和教育部博士点专项科研基金(20130131110010)资助

摘要 随着人们对于离子液体参与自组装行为的重视, 表面活性剂在其中构建溶致液晶的研究日益深入. 选择离子液体作为组装介质, 可将其优良特性引入到溶致液晶中, 从而达到改善体系性质、扩展其应用范围的目的. 本文总结了阳离子季铵盐类表面活性剂(常规单链、双链及Gemini型)、非离子表面活性剂(烷基聚氧乙醚类及植物甾醇类)及Pluronic双亲嵌段共聚物等在离子液体中自组装构建溶致液晶行为的研究进展, 用可以反映溶剂内聚能密度的Gordon参数, 对不同离子液体中形成溶致液晶的差异进行了分析, 并对该领域的发展趋势进行了展望.

关键词 离子液体, 溶致液晶, 表面活性剂, 疏溶剂作用, 氢键

作为有序分子聚集体的重要类型之一, 溶致液晶(lyotropic liquid crystal, LLC)通常是由表面活性剂和水等二元或多元组分在一定温度和浓度条件下形成的长程有序聚集结构, 相态丰富, 兼具液体的流动性和晶体的各向异性. 常见溶致液晶的相态包括层状相、六角相和立方相. 其中, 层状相液晶中表面活性剂形成的双分子层与水层相互间隔、平行排列, 形成长程有序、而短程无序的层状结构, 也叫三明治结构. 六角相液晶则是棒状聚集体平行排列形成的六方结构, 根据连续相的极性不同, 又可以分为正六角相和反六角相. 胶束立方相液晶是表面活性剂形成的球状或棒状胶束在溶液中做立方堆积, 形成的面心或体心立方结构. 而双连续立方相是由表面活性剂形成的双层膜形成两条互不相连的亲油或者亲水管道, 以无限循环方式排列堆积而成. 溶致液晶已经在纳米材料制备[1~3]、化学反应微环境[4,5]、药物载体[6~8]、润滑材料[9]、三次采油[10]和富集分离微量元素[11]等领域得到了广泛的研究和应用. 此外, 溶致液晶结构也存在于许多生物组织当中, 在生命活动中发挥着重要作用, 是研究生物膜的重要模型体系[12]. 但在研究中发现, 由水作为溶剂参与构建的溶致液晶, 存在液晶区温度范围窄、热稳定性差、电化学窗口受限和对易水解组分的限制等缺陷. 为解决这些问题, 人们一直寻求在其他非水溶剂中构建溶致液晶, 而作为一种新兴绿色溶剂的离子液体逐渐引起了人们的广泛重视.

离子液体(ionic liquids, ILs)是完全由离子组成的化合物, 理想的室温离子液体在100℃下呈液体状态. 离子液体一般是由体积较大的阳离子和体积较小的阴离子组成, 常见的阳离子有季铵盐、季鏻盐、咪唑盐和吡咯盐离子等; 阴离子有卤素离子、四氟硼酸根和六氟磷酸根离子等[13~18]. 根据其能否接受质子, 离子液体可分为质子化和非质子化离子液体两大类. 由于可供选择的离子种类和结构丰富, 离子液体的可设计性非常大, 因此也被誉为未来的溶剂[19]. 尽管种类繁多, 离子液体一般都具有熔点低、蒸汽压低、液态温度范围大、电化学窗口宽和导电导热性好等优点, 所以在许多领域都被用作溶剂, 如有机和无

引用格式: 李钦堂, 陈晓. 离子液体中构建溶致液晶. 科学通报, 2017, 62: 478–485
Li Q T, Chen X. Lyotropic liquid crystals fabricated in ionic liquids (in Chinese). Chin Sci Bull, 2017, 62: 478–485, doi: 10.1360/N972016-00374

机合成[20~23]、催化[24~26]、色谱分离[27~29]、电化学[30,31]及生物体系中[32,33]. 本文将重点介绍离子液体作为溶剂介质在表面活性剂构建溶致液晶方面的工作进展.

1 Gordon参数

Evans[34]在讨论溶剂对于表面活性剂自组装的驱动力时, 引入了Gordon参数的概念. 其定义为

$$G = \gamma / V_{\mathrm{m}}^{-1/3},$$

其中, γ 为气/液界面的表面张力, V_{m}为溶剂分子摩尔体积. Gordon参数给出了溶剂内聚能密度的衡量, 高的参数值意味着溶剂对表面活性剂组装有更强的驱动力.

水作为自组装驱动力最强的溶剂, 具有最高的Gordon参数(2.75 J m^{-3})[35]. 而丁酸乙基铵是能支持表面活性剂自组装的质子化离子液体中Gordon参数最低的[15], 只有0.576 J m^{-3}. 硝酸乙基铵(EAN)是研究最为广泛的质子化离子液体, 具有较高的Gordon参数(1.060 J m^{-3})[36], 表面活性剂在其中的聚集形态最为丰富; 而咪唑类非质子化离子液体的Gordon参数, 如1-丁基-3-甲基咪唑的四氟硼酸盐[Bmim]BF_4 (0.794 J m^{-3})[37]或六氟磷酸盐[Bmim]PF_6(0.822 J m^{-3})[37]的数值, 居于能够使表面活性剂聚集的溶剂下限, 在其中形成聚集体的形貌相对较少. 因此, 一般来说, 具有较大Gordon参数的溶剂, 能够支持形成更丰富的溶致液晶相, 且液晶相的热稳定性更好[38]. 这一点可以很好地用来指导表面活性剂自组装所用溶剂的选择.

2 离子液体中构建的溶致液晶

Evans课题组[39]在1983年就报道了二硬脂酰磷脂酰胆碱(distearoylphosphotidylcholine, DSPC)与EAN (ethylammonium nitrate)按1∶1混合形成的溶致液晶, 这是溶致液晶在离子液体介质中形成的首次报道. 但与水中的相行为比较, DSPC在EAN中聚集体形貌不够丰富, 没有层状相的形成. 这是由于EAN对烷烃链具有比水更好的溶解能力, 二者之间的相互作用使得表面活性剂的临界堆积参数(critical packing parameter, CPP)变小[40]. 随后, Tamura-Lis等人[41]将*L*-二棕榈酰磷脂酰胆碱(dipalmitoylphosphatidylcholine, DPPC)与EAN混合, 也得到了溶致液晶. 与DSPC/EAN体系不同的是, DPPC/EAN (20%, w/v)体系仅存在由多重层状相到六角状排列液晶相的单一相变, 相变温度为59.5℃. 但是在之后时间里, 以离子液体作溶剂构建溶致液晶并没有引起人们足够的重视. 直到近些年来, 这一领域的研究才逐渐增多[13~17]. 下面根据表面活性剂的类型分别介绍它们在离子液体中构建的溶致液晶.

2.1 阳离子型表面活性剂构建的溶致液晶

澳大利亚Drummond课题组[36]利用偏光显微镜下渗透扫描的观察方法, 研究了十六烷基三甲基溴化铵(hexadecyltrimethylammonium bromide, CTAB)与包括EAN在内的20多种质子化离子液体形成的二元体系, 发现凡能形成溶致液晶的体系, 按照出现的液晶相态大体可分为两类: 一类是随CTAB浓度增加, 出现了六角相、立方相和层状相的体系; 另一类则仅出现了层状相. 他们认为, 离子液体除了可以充当表面活性剂自组装的介质以外, 一些长链的离子液体还可能起到了助表面活性剂的作用. Drummond课题组[42]在研究阳离子端基含有羟基的离子液体(硝酸乙醇铵(ethanolammonium nitrate, EOAN)及甲酸二乙醇铵(diethanolammonium formate, DEOAF))对表面活性剂相行为的影响时还发现, 十六烷基三甲基氯化铵(hexadecyltrimethylammonium chloride, CTAC)和十六烷基溴化吡啶(hexadecylpyridinium bromide, HDPB)在这两种离子液体中表现出更加丰富的溶致液晶相态. 它们在EAN体系中只有六角相形成; 而在EOAN和DEOAF中, 还能观察到双连续立方相的存在. 这是由于羟基的引入使得离子液体间的氢键作用增强, 内聚能增大, 从而具有更大的Gordon参数. 这一结果也为设计具有较大Gordon参数的离子液体提供了思路.

本课题组[43]曾研究了十六烷基三甲基咪唑氯化物[C_{16}mim]Cl在EAN中的聚集行为. 该二元体系的相图如图1所示, 随着[C_{16}mim]Cl浓度的增加, 六角相、层状相和反双连续立方相溶致液晶依次形成, 并分别跨越不同的温度范围. 该体系中导致不同液晶相态形成的主要原因为疏溶剂作用和氢键作用. 与[C_{16}mim]Cl在水中的相行为比较, 在EAN中形成了水中未观察到的反双连续立方相, 这是表面活性剂与EAN及水分子之间不同的作用力所致.

山东大学郑利强课题组[44]也报道过长链甲基吡

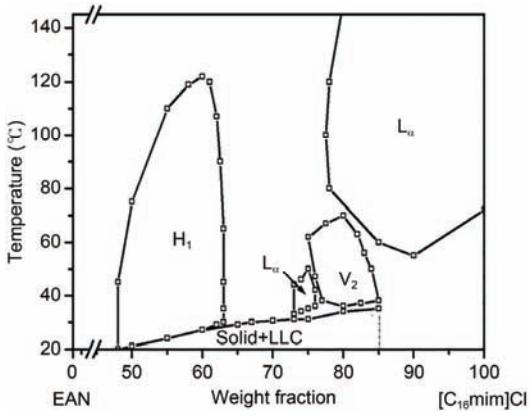

图 1 [C_{16}mim]Cl/EAN二元体系的相图[43]. 其中H_1, L_α和V_2分别表示六角相、层状相和反双连续立方相

Figure 1 Phase diagram of [C_{16}mim]Cl/EAN binary system[43]. H_1, L_α and V_2 denote the hexagonal, lamellar and reverse bicontinuous phases, respectively

咯烷类(C_{16}MPB)表面活性剂在EAN中的溶致液晶行为，并与对应的水体系做了详细比较，发现在EAN中形成的溶致液晶相区域变窄，这是由于EAN中的疏溶剂作用弱于水导致的. 差示扫描量热(DSC)考察形成液晶的热稳定性发现，在超过100℃时液晶相仍能稳定存在.

相对于研究较多的单链表面活性剂，双链表面活性剂在离子液体中的研究并不多见[45~47]. 特拉华大学Wagner课题组[45]研究了双十二烷基二甲基溴化铵(dimethyldidodecylammonium bromide, DDAB)在EAN中的聚集行为. 随着DDAB浓度增加，体系中聚集体由海绵相转变为层状相溶致液晶. 由于EAN中较弱的疏溶剂作用，所得海绵相可以在较大DDAB浓度区间稳定. 这一行为在水体系中非常少见，使得DDAB/EAN体系成为理想的海绵相模型体系.

Gemini表面活性剂是由2个表面活性剂单体通过间隔基连接而成，由于其独特的分子结构，在水中表现出丰富的相行为，但是其在离子液体中的聚集行为研究较少. 本课题组[48]率先研究了季铵盐类Gemini表面活性剂*m*-2-*m*(*m*=10, 12, 14)在EAN中的相行为，并与其在水中的情形进行了比较. *m*-2-*m*分子可以在EAN中聚集形成胶束相、两相共存区以及反六角相溶致液晶，结构如图2所示. EAN 体系中的三维氢键网络结构是Gemini分子能够进行自组装的基础，由此产生的疏溶剂作用是液晶相形成的主要驱动力. 相对于水体系，EAN体系表现出两个独特的性质: 一是室温熔盐的离子特性，产生的电荷屏蔽作用使得Gemini分子的头基可以更加靠近; 二是较水中更弱的疏溶剂作用，对烷基链的溶解度较大，使得表面活性剂疏溶剂部分的体积增大. 正是这些差异，导致了Gemini分子在水与EAN中聚集行为的不同. 与此同时，本课题组[49]还研究了不对称链长的Gemini表面活性剂*m*-2-*n*(*m*+*n*=24, *m*=16, 14, 12)在EAN中的聚集行为. 随着分子不对称性的增大，*m*-2-*n*形成反六角相的起始浓度减低，所得液晶相的黏弹性及热稳定性均增强. 这表明随着分子不对称性的增大，分子的疏溶剂作用逐渐增强.

此外，本课题组[50]还研究了质子化离子液体(PILs)结构变化对Gemini表面活性剂12-2-12相行为的影响. 与EAN相比，质子化离子液体的阳离子碳链长度增加1或2个亚甲基，即硝酸丙基铵(propylammonium nitrate, PAN)和硝酸丁基铵(butylammonium nitrate, BAN)，将引起液晶相结构的“反转”(图2). 在12-2-12/PAN体系中，可以观测到正六角相; 而在BAN体系中，正六角相、双连续立方相、层状相依次出现. 上述聚集行为的变化是由于PAN和BAN疏溶剂作用进一步减弱，更容易参与到12-2-12的组装之中，使得12-2-12的有效分子头基占据面积显著增大，从而形成曲率更大的聚集体. 离子液体这样的调控作用在单链表面活性剂(十二烷基三甲基溴化铵)及不对称Gemini表面活性剂(16-2-8)体系中并没有发现，说明12-2-12的独特分子结构在这里也起到重要作用.

2.2 非离子表面活性剂构建的溶致液晶

悉尼大学Araos和Warr[51]研究了烷基聚氧乙烯醚型表面活性剂C_nE_m在EAN中的相行为，发现C_nE_m表现出与水中类似的聚集性能. 但在EAN中，为了得到与水中相同温度及浓度区间的液晶相，表面活性

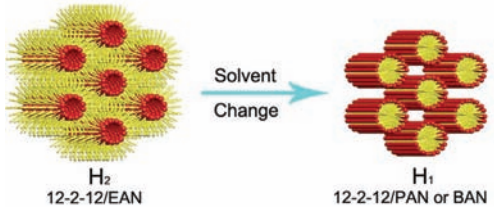

图 2 (网络版彩色)溶剂结构改变引起 12-2-12/PILs体系六角相液晶结构的反转行为[50]. 其中H_2代表反六角相

Figure 2 (Color online) The hexagonal phase transition induced by solvent structure changes in 12-2-12/PILs systems[50]. H_2 donates the reverse hexagonal phase

剂的烷基链需要更长，如$C_{16}E_8$/EAN体系才与$C_{14}E_8$/水体系的相行为较为接近. 另外，烷基链及聚氧乙烯醚链长的变化对相行为的影响在EAN和水中保持一致. 而后，Atkin等人[52]又研究了C_nE_m在硝酸丙基铵(PAN)中的相行为，发现随着离子液体中阳离子上烷基链的增长，PAN的Gordon参数下降，对表面活性剂烷基链的溶解力增强，疏溶剂作用进一步减弱. 因此在PAN中，液晶相的种类更少，聚集体的曲率也增加.

Drummond课题组[53]考察了表面活性剂myverol 18-99K(主要成分是单甘油油酸酯, monoolein)和植烷三醇(phytantriol)在多种质子化离子液体中的聚集行为，并绘制了这些体系形成溶致液晶的相图，将这些二元体系形成的液晶种类大致分为4种类型：层状相和反立方相、仅层状相、反六角相和反立方相和仅反六角相. 研究表明，质子化离子液体的种类极大地影响了形成的溶致液晶结构类型.

本课题组[54]研究聚氧乙烯月桂醚(Brij 97)在一系列离子液体中的相行为时发现，只有在EAN中能够形成六角相溶致液晶. 通过对液晶相结构的小角X射线散射分析得知，Brij 97分子在液晶相中不是完全伸展，而是以一定的弯曲度排列. EAN则主要分散在聚氧乙烯嵌段之间，并且形成了N-H···O$(CH_2)_2$，N-H···O-NO_2，N-H···N-H，N-H···O-H，O-H···O-NO_2和O-H···O$(CH_2)_2$等类型的氢键网络，从而促进了溶致液晶的形成. 通过图3展示的不同离子液体中Brij 97相态分布图进行比较，可以看出，从H_2O到EAN到[Bmim]PF_6, [Bmim]BF_4，硝酸吡咯烷基铵[Pyrr][NO_3]和丁酸乙基铵EAB, Brij 97在其中构建有序分子聚集体的能力逐渐减弱，与这些溶剂Gordon参数依次变小的顺序一致. 由此还可以看出，质子化离子液体由于能够形成氢键网络，一般具有较强的驱动力；而增加其中阴离子烷基链的长度，也会降低溶剂对聚集的驱动力.

甾醇聚氧乙烯醚类表面活性剂(BPS-*n*，*n*为乙氧基个数)是以甾核为疏溶剂部分、聚氧乙烯链为亲溶剂头基的非离子表面活性剂. 与传统的C_nE_m分子相比，其疏溶剂部分具有刚性较强、体积大的特点，所构建聚集体也体现出刚性的特点. 东京理工大学Sakai课题组[55,56]研究了此类表面活性剂在非质子化离子液体[Bmim]PF_6中的相行为，发现BPS-20能够形成胶束立方相、六角相和层状相. 减少EO链长度，体系只会出现低曲率的层状相，而增加EO链的长度，则只有胶束立方相和层状相.

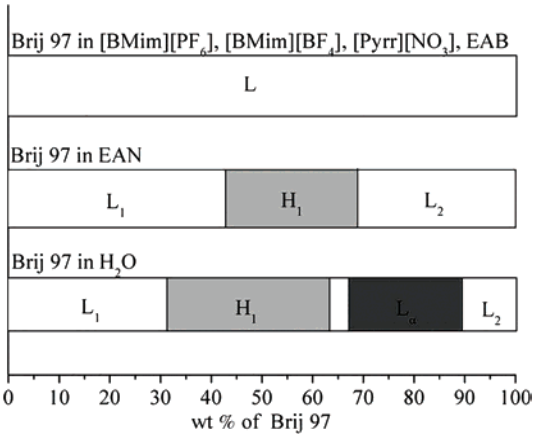

图3 25℃时Brij 97在水、EAN和其他离子液体中的相行为[54]. L_2，反胶束相; L，各向同性溶液

Figure 3 Phase behaviors of Brij 97 in water, EAN and other ILs at 25°C[54]. L_2 and L donate the reverse micellar phase and isotropic solution

本课题组[57,58]也比较了BPS-*n*分别在非质子化的[Bmim] BF_4和质子化的EAN两种离子液体中的聚集行为，所形成聚集体的形态分布如图4所示. 传统C_nE_m型分子在离子液体中主要通过氢键作用而聚集，而在氢键网络较差的咪唑类离子液体中，很难发现溶致液晶的形成，当水加入时，则会促进Brij 97形成溶致液晶[54,59]. 甾环之间则存在较强的疏溶剂相互作用，使其成为此类表面活性剂聚集的主要驱动力. 例如，BPS-10分子在聚集体中的分子排列比传统表面活性剂更为紧密，使BPS-10/[Bmim]BF_4体系中的层状相表现出很高的粘度. 表面活性剂溶剂化作用的不同，也会影响BPS-*n*表面活性剂的相行为. 与上面提到BPS-n/[Bmim]PF_6体系比较，立方相在[Bmim]BF_4体系中较少出现，因为氧乙烯链在其中的溶剂化作用比在[Bmim]PF_6中更强，其有效头基面积也会增大，导致BPS-20在[Bmim]BF_6形成具有较小堆积参数的聚集体.

与在[Bmim]BF_4中只有层状相的形成相比，当溶剂换为具有更大Gordon参数的EAN时，BPS-10体系中依次出现六角相、六角相和层状相的两相共存区、以及层状相[58]. 与[Bmim]BF_4相比，EAN中可形成类似水分子的较强的氢键网络结构，这导致 BPS-10更易聚集形成溶致液晶，并且相态较[Bmim]BF_4中更为丰富. 而EAN与EO链间的氢键作用，使形成的溶致液晶相具有更高的黏度，表现出不同的流变行为.

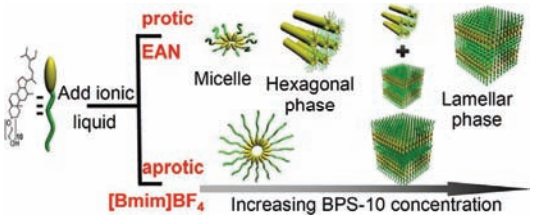

图 4 (网络版彩色)BPS-10 在EAN和[Bmim]BF_4中的相行为[57]

Figure 4 (Color online) Phase behaviors of BPS-10 in EAN and [Bmim]BF_4[57]

2.3 双亲嵌段共聚物构建的溶致液晶

本课题组[60]还率先研究了聚氧乙烯-聚氧丙烯-聚氧乙烯(PEO-PPO-PEO)双亲性三嵌段聚合物P123在[Bmim]PF_6中的溶致液晶相行为. 当P123浓度为38%~52%和65%~87%(质量分数)时, 偏光显微镜和小角X射线散射结果表明, 体系中形成六角相和层状相溶致液晶. 与相同浓度的水体系中液晶相比较[61], 此体系中形成的液晶相结构参数明显较小, 这也是因为[Bmim]PF_6密度较大, 使极性区的体积变小所致. 提出的溶致液晶形成机理如图5所示, PEO嵌段形成亲溶剂区, 而PPO嵌段形成疏溶剂区. 在驱动力方面, PEO嵌段的端基羟基能够和$[PF_6]^-$形成氢键, 离子液体的咪唑阳离子($-N^+$)与EO基团中氧原子上的孤对电子之间也可发生作用, 这两种效应与疏溶剂作用相协调, 有利于体系中长程有序结构的形成. 另外, $[Bmim]^+$含有较短的疏水丁基, 可以起到助表面活性剂的作用, 与嵌段共聚物协同形成极性/非极性界面, 增强了结构的有序性. 当然, 离子液体作为熔融盐, 对非离子表面活性剂体系的盐析效应也有助于形成自组装有序结构.

而后本课题组[62]研究了P123在EAN中的聚集行为, 该二元体系的相图如图6所示, P123可以在EAN中自组装形成胶束立方相、六角相、层状相和反双连续立方相等一系列溶致液晶相态. 有序结构的出现是EAN对聚合物中PEO和PPO两种嵌段作用能力不同的结果. 与[Bmim]PF_6相比, P123在EAN中能形成胶束立方相和反双连续立方相两种立方相, 这与先前提到的质子化离子液体自身能够形成氢键网络有关, 这使它们较非质子化溶剂具有更强的自组装促进能力, 所以P123在EAN中表现出更丰富的相行为. 而与水中情形比较, P123在EAN中能形成反双连续立方相. 因为EAN通过$CH_3CH_2NH_3^+$与氧乙烯基团之间形成氢键, 从而对PEO嵌段产生了较强的作用, 这

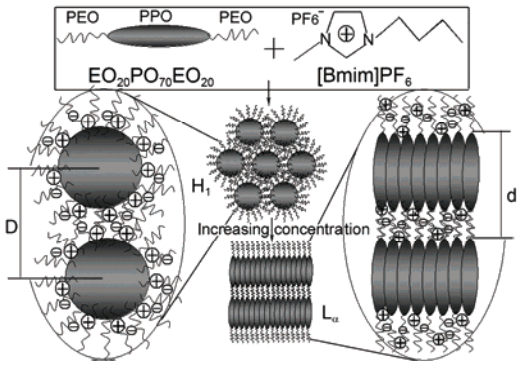

图 5 P123/[Bmim]PF_6体系中溶致液晶形成机理图[60]

Figure 5 Aggregation mechanism of LLCs in P123/[Bmim]PF_6 system[60]

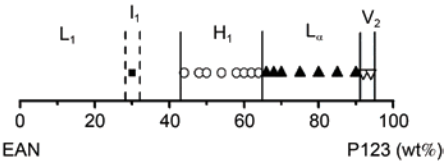

图 6 25℃时P123/EAN体系的二元相图[62]

Figure 6 The P123/EAN binary phase diagram at 25℃[62]

进一步加大了PEO和PPO嵌段的分隔, 导致聚集体形成. 由于EAN对极性基团PEO嵌段的溶剂化能力弱, 而对疏水区PPO嵌段的亲合力强, 这有可能使得P123的有效头基占据面积变小而疏溶剂体积增大, 从而形成反双连续立方相.

3 结论与展望

本文主要介绍了表面活性剂在离子液体中构建溶致液晶的研究进展. 尽管离子液体对表面活性剂的烷基链具有较强的溶解力, 使之表现出比水弱的疏溶剂作用, 但依然能够支持表面活性剂分子在其中的自组装行为. 通过目前开展的工作可以看出, 此类研究的重点集中在阳离子表面活性剂在质子化离子液体、非离子表面活性剂及嵌段共聚物在质子化和非质子化离子液体中的溶致液晶行为. 因此, 今后的研究重点可能集中在以下几个方面: (1) 合成新型离子液体. 根据离子液体在作为自组装介质方面的构效关系, 设计特定需求的离子液体; (2) 设计新型表面活性剂. 新型表面活性剂在离子液体中也许会表现出与水中不相一致的相行为, 如Gemini型、Bola型、含氟或含硅表面活性剂、及超分子表面活性剂等; (3) 扩展新的溶致液晶体系. 如阳离子表面活性剂在非质子化离子液体中, 两性表面活性剂的离子液体体

系等. 值得一提的是, 阴离子表面活性剂在离子液体中构建的溶致液晶尚未见报道, 可能与溶解度低有关. 考虑到其能在离子液体中形成胶束[17], 阴离子表面活性剂随其浓度增加的进一步组装还是值得尝试的.

参考文献

1 Attard G S, Goeltner C G, Corker J M, et al. Liquid-crystal templates for nanostructured metals. Angew Chem Int Ed, 1997, 36: 1315–1317
2 Attard G S, Leclerc S A A, Maniguet S, et al. Mesoporous Pt/Ru alloy from the hexagonal lyotropic liquid crystalline phase of a nonionic surfactant. Chem Mater, 2001, 13: 1444–1446
3 Bartlett P N, Gollas B, Guerin S, et al. The preparation and characterisation of H-1-e palladium films with a regular hexagonal nanostructure formed by electrochemical deposition from lyotropic liquid crystalline phases. Phys Chem Phys Chem, 2002, 4: 3835–3842
4 Lv F F, Chen B, Wu L Z, et al. Enhanced stereoselectivity in photoelectrocyclization of tropolone ethers via confinement in chiral inductor-modified lyotropic liquid crystals. Org Lett, 2008, 10: 3473–3476
5 Lv F F, Li X W, Wu L Z, et al. Photochemical reaction of cyclohexyl phenyl ketone within lyotropic liquid crystals. Tetrahedron, 2008, 64: 1918–1923
6 Gin D L, Lu X Y, Nemade P R, et al. Recent advances in the design of polymerizable lyotropic liquid-crystal assemblies for heterogeneous catalysis and selective separations. Adv Funct Mater, 2006, 16: 865–878
7 Guo C, Wang J, Cao F, et al. Lyotropic liquid crystal systems in drug delivery. Drug Discov Today, 2010, 15: 1032–1040
8 Negrini R, Mezzenga R. pH-Responsive lyotropic liquid crystals for controlled drug delivery. Langmuir, 2011, 27: 5296–5303
9 Ma C S, Li G Z, Shen Q A. Study of lyotropic liquid crystal in lubrication on aluminum alloy surfaces. J Dispersion Sci Technol, 1999, 20: 1025–1030
10 Zheng M Y, Wang Z W, Liu F, et al. Study on the microstructure and rheological property of fish oil lyotropic liquid crystal. Colloids Surf A, 2011, 385: 47–54
11 Liu X X, Yang Q W, Bao Z B, et al. Nonaqueous lyotropic ionic liquid crystals: Preparation, characterization, and application in extraction. Chem Eur J, 2015, 21: 9150–9156
12 Siegel D P. The modified stalk mechanism of lamellar/inverted phase transitions and its implications for membrane fusion. Biophys J, 1999, 76: 291–313
13 Hao J C, Zemb T. Self-assembled structures and chemical reactions in room-temperature ionic liquids. Curr Opin Colloid Interface Sci, 2007, 12: 129–137
14 Greaves T L, Drummond C J. Protic ionic liquids: Properties and applications. Chem Rev, 2008, 108: 206–237
15 Greaves T L, Drummond C J. Ionic liquids as amphiphile self-assembly media. Chem Soc Rev, 2008, 37: 1709–1726
16 Greaves T L, Drummond C J. Solvent nanostructure, the solvophobic effect and amphiphile self-assembly in ionic liquids. Chem Soc Rev, 2013, 42: 1096–1120
17 Greaves T L, Drummond C J. Protic ionic liquids: Evolving structure-property relationships and expanding applications. Chem Rev, 2015, 115: 11379–11448
18 Hayes R, Warr G G, Atkin R. Structure and nanostructure in ionic liquids. Chem Rev, 2015, 115: 6357–6426
19 Rogers R D, Seddon K R. Ionic liquids-solvents of the future? Science, 2003, 302: 792–793
20 Welton T. Room-temperature ionic liquids. Solvents for synthesis and catalysis. Chem Rev, 1999, 99: 2071–2083
21 Holbrey J D, Seddon K R. Ionic liquids. Clean Prod Proc, 1999, 1: 223–236
22 Yong Z, Schattka J H, Antonietti M. Room-temperature ionic liquids as template to monolithic mesoporous silica with wormlike pores via a sol-gel nanocasting technique. Nano Lett, 2004, 4: 477–481
23 Wang Y, Yang H. Synthesis of CoPt nanorods in ionic liquids. J Am Chem Soc, 2005, 127: 5316–5317
24 Wasserscheid P, Keim W. Ionic liquids-new “solutions” for transition metal catalysis. Angew Chem Int Ed, 2000, 74: 157–189
25 Zhao D B, Wu M, Kou Y, et al. Ionic liquids: Application in catalysis. Catal Today, 2002, 74: 157–189
26 Dupont J, de Souza R F, Suarez P A Z. Ionic liquid (molten salt) phase organometallic catalysis. Chem Rev, 2002, 102: 3667–3692
27 Domanska U, Bogel-Lukasik E, Bogel-Lukasik R. Solubility of 1-dodecyl-3-methylimidazolium chloride in alcohols (C_2-C_{12}). J Phys Chem B, 2003, 107: 1858–1863
28 Scurto A M, Aki S N V K, Brennecke J F. Carbon dioxide induced separation of ionic liquids and water. Chem Commun, 2003, (5): 572–573
29 Swatloski R P, Visser A E, Reichert W M, et al. Solvation of 1-butyl-3-methylimidazolium hexafluorophosphate in aqueous ethanol—A green solution for dissolving “hydrophobic” ionic liquids. Chem Commun, 2001, (20): 2070–2071
30 Lagrost C, Carrie D, Vaultier M, et al. Reactivities of some electrogenerated organic cation radicals in room-temperature ionic liquids: Toward an alternative to volatile organic solvents? J Phys Chem A, 2003, 107: 745–752
31 Buzzeo M C, Evans R G, Compton R G. Non-haloaluminate room-temperature ionic liquids in electrochemistry—A review. Chem Phys Chem, 2004, 5: 1106–1120

32 Kumar A, Venkatesu P. Overview of the stability of α-chymotrypsin in different solvent media. Chem Rev, 2012, 112: 4283–4307
33 Mood S H, Golfeshan A H, Tabatabaei M, et al. Lignocellulosic biomass to bioethanol, a comprehensive review with a focus on pretreatment. Renew Sust Energ Rev, 2013, 27: 77–93
34 Evans D F. Self-organization of amphiphiles. Langmuir, 1988, 4: 3–12
35 Beelsey A H, Evans D F, Laughlin R G. Evidence for the essential role of hydrogen bonding in promoting amphiphilic self-assembly: Measurements in 3-methylsydnone. J Phys Chem, 1988, 92: 791–793
36 Greaves T L, Weerawardena A, Fong C, et al. Many protic ionic liquids mediate hydrocarbon-solvent interactions and promote amphiphile self-assembly. Langmuir, 2007, 23: 402–404
37 Huddleston J G, Visser A E, Reichert W M, et al. Characterization and comparison of hydrophilic and hydrophobic room temperature ionic liquids incorporating the imidazolium cation. Green Chem, 2001, 3: 156–164
38 Auvray X, Perche T, Petipas C, et al. Influence of solvent-headgroup interactions on the formation of lyotropic liquid crystal phases of surfactants in water and nonaqueous protic and aprotic solvents. Langmuir, 1992, 8: 2671–2679
39 Evans D F, Kaler E W, Benton W J. Liquid crystals in a fused salt: β,γ-distearoylphophotidylcholine in *N*-ethylammonium nitrate. J Phys Chem, 1983, 87: 533–535
40 Israelachvili J N. Intermolecular and Surface Forces. San Diego: Academic Press, 1992
41 Tamura-Lis W, Lis L J, Quinn P J. Structures and mechanisms of lipid phase transitions in nonaqueous media: Dipalmitoylphosphatidylcholine in fused salt. J Phys Chem, 1987, 91: 4625–4627
42 Chen Z F, Greaves T L, Fong C, et al. Lyotropic liquid crystalline phase behaviour in amphiphile-protic ionic liquid systems. Phys Chem Chem Phys, 2012, 14: 3825–3836
43 Zhao Y R, Chen X, Wang X D. Liquid crystalline phases self-organized from a surfactant-like ionic liquid C_{16}mimCl in ethylammonium nitrate. J Phys Chem B, 2009, 113: 2024–2030
44 Zhao M W, Gao Y A, Zheng L Q. Liquid crystalline phases of the amphiphilic ionic liquid *N*-hexadecyl-*N*-methylpyrrolidinium bromide formed in the ionic liquid ethylammonium nitrate and in water. J Phys Chem B, 2010, 114: 11382–11389
45 Lopez-Barron C R, Basavaraj M G, De Rita L, et al. Sponge-to-lamellar transition in a double-tail cationic surfactant/protic ionic liquid system: Structural and rheological analysis. J Phys Chem B, 2012, 116: 813–822
46 Lopez-Barron C R, Li D C, De Rita L, et al. Spontaneous thermoreversible formation of cationic vesicles in a protic ionic liquid. J Am Chem Soc, 2012, 134: 20728–20732
47 Lopez-Barron C R, Wagner N J. Structural transitions of CTAB micelles in a protic ionic liquid. Langmuir, 2012, 28: 12722–12730
48 Wang X D, Chen X, Zhao Y R, et al. Nonaqueous lyotropic liquid-crystalline phases formed by Gemini surfactants in a protic ionic liquid. Langmuir, 2012, 28: 2476–2484
49 Wang X D, Li Q T, Chen X, et al. Effects of structure dissymmetry on aggregation behaviors of quaternary ammonium Gemini surfactants in a protic ionic liquid EAN. Langmuir, 2012, 28: 16547–16554
50 Li Q T, Wang X D, Yue X, et al. Phase transition of a quaternary ammonium Gemini surfactant induced by minor structural changes of protic ionic liquids. Langmuir, 2014, 30: 1522–1530
51 Araos M U, Warr G G. Self-assembly of nonionic surfactants into lyotropic liquid crystals in ethylammonium nitrate, a room-temperature ionic liquid. J Phys Chem B, 2005, 109: 14275–14277
52 Atkin R, Bobillier S M C, Warr G G. Propylammonium nitrate as a solvent for amphiphile self-assembly into micelles, lyotropic liquid crystals, and microemulsions. J Phys Chem B, 2010, 114: 1350–1360
53 Greaves T L, Weerawardena A, Fong C, et al. Formation of amphiphile self-assembly phases in protic ionic liquids. J Phys Chem B, 2007, 111: 4082–4088
54 Ma F M, Chen X, Zhao Y R, et al. A nonaqueous lyotropic liquid crystal fabricated by a polyoxyethylene amphiphile in protic ionic liquid. Langmuir, 2010, 26: 7802–7807
55 Sakai H, Saitoh T, Misono T, el al. Nonionic surfactant mixtures in an imidazolium-type room-temperature ionic liquid. J Oleo Sci, 2011, 60: 563–567
56 Sakai H, Saitoh T, Misono T, et al. Phase behavior of phytosterol ethoxylates in an imidazolium-type room-temperature ionic liquid. J Oleo Sci, 2012, 61: 135–141
57 Yue X, Chen X, Li Q T. Comparison of aggregation behaviors of a phytosterol ethoxylate surfactant in protic and aprotic ionic liquids. J Phys Chem B, 2012, 116: 9439–9444
58 Yue X, Chen X, Wang X D, et al. Lyotropic liquid crystalline phases formed by phyosterol ethoxylates in room-temperature ionic liquids. Colloids Surf A, 2011, 392: 225–232
59 Wang Z N, Liu F, Gao Y, et al. Hexagonal liquid crystalline phases formed in ternary systems of Brij 97-water-ionic liquids. Langmuir, 2005, 21: 4931–4937
60 Wang L Y, Chen X, Chai Y C, et al. Lyotropic liquid crystalline phases formed in an ionic liquid. Chem Commun, 2004, (24): 2840–2841
61 Holmqvist P, Alexandridis P, Lindman B. Modification of the microstructure in block copolymer-water-“oil” systems by varying the copolymer composition and the “oil” type: Small-angle X-ray scattering and deuterium-NMR investigation. J Phys Chem B, 1998, 102: 1149–1158
62 Zhang G D, Chen X, Zhao Y R, et al. Lyotropic liquid-crystalline phases formed by Pluronic P123 in ethylammonium nitrate. J Phys Chem B, 2008, 112: 6578–6584

Summary for “离子液体中构建溶致液晶”

Lyotropic liquid crystals fabricated in ionic liquids

LI QinTang & CHEN Xiao*

Key Laboratory of Colloid and Interface Chemistry, Ministry of Education, Shandong University, Jinan 250100, China
* Corresponding author, E-mail: xchen@sdu.edu.cn

The lyotropic liquid crystals (LLCs) are one important kind of aggregates formed by surfactants in solvent media and have wide applications in nanomaterial systhesis, chemical reaction environment, drug delivery, lubricating material, oil recovery and so on. Meanwhile, the ionic liquids (ILs) have currently widely used as novel nonaqueous media in the areas of organic synthesis and catalysis, biochemical engineering, materials science, electrochemistry, carbohydrate chemistry, and separation techniques for their unique characteristics of low melting temperature, negligible vapor pressure, wide electrochemical window, nonflammability, good catalytic properties, high thermal stability, and ionic conductivity. For these reasons, more and more attention has been paid to ILs as the self-assembly media. Among them, the LLCs formed by surfactants in ILs have received increasingly studies. Exploration on the LLC behaviors of surfactants in ILs may provide not only a better understanding of intermolecular actions in self-assembly, but also certain new properties to LLCs, like better thermostability compared to those constructed in aqueous media. For these reasons, this account here reviews the LLC phase behaviors in ILs of various surfactants, including quarternary ammonium cationic surfactant, alkyl polyoxyethylene nonionic surfactant and Pluronic block copolymer. For the cationic surfactants, several single chain molecules like the hexadecyltrimethylammonium bromide, 1-hexadecyl-3-methylimidazolium chloride, and N-hexadecyl-N-methylpyrrolidinium bromide, their phase behaviors in various ILs were summaried. Various LLC phases including the normal hexagonal, lamellar, and reverse bicontinuous cubic LLC phases could be detected in ethylammonium nitrate (EAN). The hexagonal LLC phase with better thermostability was formed in EAN compared to that in water. For the molecule with two alkyl chains on one head, the dimethyldidodecylammonium bromide, the sponge and lamellar phases were observed in EAN and the sponge phase could be extended to larger region than that in aqueous system. Unlike the single chain surfactants, the reverse hexagonal phases were observed in the quarternary ammonium Gemini surfactants/EAN systems, which were not observed in corresponding water media. With increasing the chain length of one or two ethylene groups in cation of EAN, that is, from EAN to PAN or BAN, the normal LLC phases were formed back. As for the polyoxyethylene nonionic surfactants (C*n*E*m*) in EAN, their phase behaviors were similar to those in water. Due to the weaker solvophobic interactions in EAN than in water, the longer alkyl chains were necessary for the formation of LLC. While in aprotic ILs, no LLC phase was observed. However, for the phytosterol ethoxylate surfactants (BPS-n), the LLC phases were observed both in EAN and also in aprotic ILs like [Bmim]BF_4 and [Bmim]BF_6. Similar aggregation behaviors were also observed for Pluronic block copolymer in EAN and [Bmim]BF_4. The difference in phase behaviors of these surfactants in various ILs was analyzed by Gordon parameter, which was a measure of the cohesive energy density of the solvent. Generally speaking, ILs with higher Gordon parameters are correspondent to greater LLC diversity and better thermostability. The protic ionic liquids, which are capable of accepting protons and form hydrogen bonding network, would have a stronger ability of supporting surfactant self-assembly than the aprotic ionic liquids. This is the reason why richer phases are usually formed in EAN than in [Bmim]BF_4 and [Bmim]BF_6. Based on the review, the perspective for future research in this area has been also provided, such as synthesis of novel kinds of ILs and surfactants and investigation on new self-assembly systems.

ionic liquid, lyotropic liquid crystal, surfactant, solvophobic interaction, hydrogen bonding

doi: 10.1360/N972016-00374